UDC 541.6:547.1:546.711:543.422

3,3′-DIHYDROXY-4,4′-[1,2-CYCLOHEXANEDIYL BIS(NITRILOMETHYLIDYNE)]-BIS-PHENOL SCHIFF-BASE AND ITS Mn(II) COMPLEX: SYNTHESIS, EXPERIMENTAL AND THEORETICAL CHARACTERIZATION

H. Eshtiagh-Hosseini[1], S.A. Beyramabadi[2], M. Mirzaei[1], A. Morsali[2], A.R. Salimi[1], M.A. Naseri[3]

[1]*Department of Chemistry, Ferdowsi University of Mashhad, Mashhad, Iran*
 E-mail: heshtiagh@um.ac.ir
[2]*Department of Chemistry, Mashhad branch, Islamic Azad University, Mashhad, Iran*
 E-mail: beiramabadi6285@mshdiau.ac.ir
[3]*Department of Chemistry, Faculty of Science, Birjand University, Birjand, Iran*

In this work, a 3,3′-dihydroxy-4,4′-[1,2-cyclohexanediyl bis (nitrilomethylidyne)]-bis-phenol [=H_2L] Schiff-base ligand and its Mn(II) complex [$Mn(L)(H_2O)_2$] are newly synthesized and characterized by elemental analysis, IR and NMR spectroscopies. Also the geometry optimizations, assignment of the IR bands and NMR chemical shifts are computed using the density functional theory (DFT) method. The DFT optimized geometry of the ligand is not planar; each of the cyclohexane and two benzene rings are located in separate planes. The phenolic protons are engaged in the intramolecular-hydrogen-bonding interactions with azomethine nitrogen atoms. In the optimized geometry of the octahedral Mn^{2+} complex, the dianionic L^{2-} acts as a tetradentate ligand in the N, N, O^-, O^- manner, where the coordinating atoms occupy the four equatorial positions. The two axial positions are occupied by two H_2O ligands. The theoretical and experimental results are in good agreement, confirming the validity of the optimized geometries for the H_2L ligand and its Mn complex.

K e y w o r d s : Schiff base, salen, Mn, DFT, IR assignment, NMR, cyclohexanediyl.

INTRODUCTION

In order to mimic active intermediates in enzyme-catalyzed oxidation reactions, metalloporphyrin and metallosalen complexes [salen = N,N′-bis(salicylidine)ethylenediaminato)] of iron, manganese, chromium, and ruthenium have been used as model compounds and have been shown to be capable of catalyzing oxygen atom transfer from some monooxygen sources to saturated and unsaturated hydrocarbons and other organic substrates. Hence, within the last two decades, syntheses of salen and salophen ligands along with their complexes have received more attention, mainly because of their extensive applications, especially in the field of biochemistry and catalyses [1—4].

Transition metal salen complexes are recognized as powerful homogeneous catalysts in the oxidation reactions by various single oxygen atom donors such as NaClO, PhIO, $KHSO_5$, H_2O_2, and $NaIO_4$. Water-soluble Schiff base complexes have mainly been used as DNA cleavage catalysts [5—11].

We have initiated a systematic study on the transition metal complexes, including salen- type ligands by taking Co, Cu, and Fe as metal ions. We also have reported their DFT computational studies for better understanding of the structures of respective complexes [12—15]. In continuation of our previous works on the chemistry of salen complexes of transition metals, herein we report the theoretical investigation on a new Schiff-base ligand, namely 3,3′-dihydroxy-4,4′-[1,2-cyclohexane-

diylbis(nitrilomethylidyne)]-bis-phenol together with its Mn(II) complex under normal reaction conditions. The validity of the optimized structures has been evaluated by comparing the DFT and experimental results.

EXPERIMENTAL

Materials and methods. All of the used chemicals were purchased from Merck Company and used without further purification. Melting points were determined using an electrothermal 9100 melting point apparatus. The IR spectra were recorded on a Buck 500 infrared spectrophotometer using KBr discs. Elemental analysis (C, H, N) was performed on a Heraeus elemental analyzer CHN-O-Rapid. ^{1}H and ^{13}C NMR spectra were obtained on a Bruker Drx-500 Avance spectrometer (500.13 MHz) with $(CD_3)_2CO$ as a solvent.

Synthesis of the H$_2$L ligand (C$_{20}$H$_{20}$N$_2$O$_4$). A solution of 0.75 g (6.66 mmol) cyclohexane-1,2-diamine and 1.88 g (13.61 mmol) of dihydroxybenzaldehyde in toluene (150 ml) was refluxed under vigorous stirring with a Dean-Stark for 3 h. The resulting suspension was kept at room temperature prior to being filtered, washed with ethanol (2×10 ml), and dried with diethyl ether (2×10 ml) to afford an orange solid. The solid was recrystallized for further purification. (Yield: 82 %, m.p. > 250 °C).

Synthesis of the Mn^{II} complex ([MnC$_{22}$H$_{26}$N$_2$O$_6$]). To a hot solution of MnCl$_2$·6H$_2$O (0.01 g, 0.06 mmol) a warm methanolic solution (10 ml) of 3,3′-dihydroxy-4,4′-[1,2-cyclohexanediyl bis(nitrilomethylidyne)]-bis-phenol (L1) (0.02 g, 0.06 mmol) was added and refluxed for 3 h at room temperature. The orange microcrystalline solid of the product was washed with chloroform and diethyl ether and dried under vacuum. Yield: 45 %, m.p. > 300 °C, % anal. Calcd. (Found) for [Mn L(H$_2$O)$_2$] or C$_{20}$H$_{22}$N$_2$O$_6$Mn, Mw = 440 g/mol: C, 54.54 (52.95); H, 5.90 (5.96); N, 6.36 (6.17).

Computational details. All calculations have been performed using DFT with the B3LYP functional [16], as implemented in the GAUSSIAN 98 program package [17]. The 6-311+G(*d*,*p*) basis set was employed, except for Mn atom for which the LANL2DZ basis set [18] was used with including effective core potential functions.

Firstly, the geometries of the H$_2$L ligand and its Mn complex were fully optimized. The gas phase optimized geometries were confirmed to have no imaginary frequency of the Hessian, which then were used for the theoretical evaluation of vibrational frequencies of the ligand and the complex. In addition, the ^{1}H and ^{13}C NMR chemical shifts of H$_2$L were predicted at the same computational level with respect to tetramethylsilane (TMS). Here, the GIAO method was used for the prediction of DFT nuclear shieldings [19].

The DFT vibrational frequencies are usually higher than the experimental ones, which can be corrected by applying the procedure of scaling the wavenumbers. Here, the scale factor of 0.9614 was used for the calculated wavenumbers [20].

RESULTS AND DISCUSSION

Geometry optimization. Theoretical calculations could be considered as complementary to or the replacement for experimental methods in the determination of their structural parameters [11—15, 21—24]. Here, the structural parameters of the H$_2$L ligand and its Mn(II) complex have been theoretically computed. The obtained results are in agreement with the structural data reported for the similar Schiff-base ligands [25—28] and complexes [29—35]. Optimized geometries of the investigated ligand and complex with their atomic labeling are shown in Figs. 1 and 2 respectively. Molecular structure visualizations were made using the Chemdraw [36] and Chemcraft [37] programs.

As shown in Fig. 1, the benzene rings are essentially planar in the optimized geometry of H$_2$L. However, these aromatic rings lie in separate planes which make a dihedral angle of approximately 50.0° to each other. The calculated C4—C5—C8—C9, C2—C1—C12—C11, and C3—C6—C13—C10 dihedral angles are 39.9°, 41.7°, and 47.3° respectively. The C=C bond distances (138.5—142.7 pm) of these rings are in the expected range [38].

In the diamine-bridge region, the cyclohexane ring has a *boat* form, which is in a separate plane toward the benzene rings. As expected, the C—C—C angles in the benzene rings and the cyclohexane
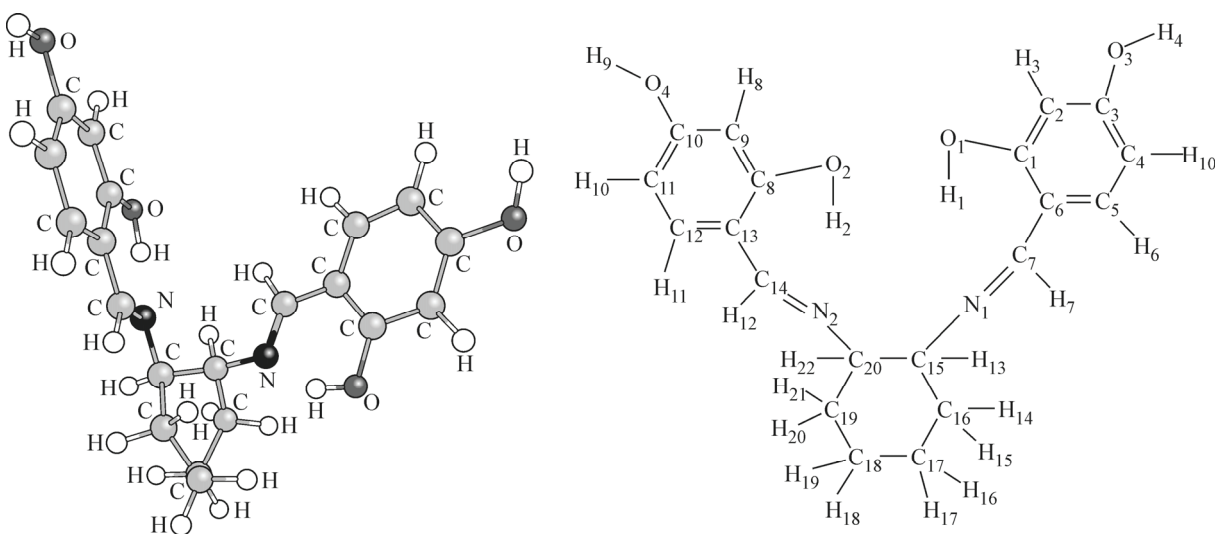
Fig. 1. Structure and B3LYP optimized geometry of the H_2L ligand together with its labeling

ring are about 120° and 110° respectively, where the carbon-carbon bond lengths are about 140 pm and 154 pm respectively. The calculated C15—C16—C17—C18 and C16—C15—C19—C20 dihedral angles of cyclohexane ring are –36.1° and 62.5° respectively.

The resorcinol OH groups are in the same plane with the benzene ring. For example, the C3—C2—C1—O1 and C2—C1—O1—H1 dihedral angles are –179.9° and –179.4° respectively. Also, the C1—C2—C3—O3 and C2—C3—O3—H4 dihedral angles are 180.0° and 179.8° respectively, which are 179.8° and 179.5° in the Mn complex respectively.

In free H_2L, the H1 and H2 atoms are engaged in intramolecular hydrogen bonds with the N1 and N2 atoms respectively, forming two six-membered rings. The calculated N…H hydrogen bond length and N—O distance are 169.5 pm and 260.9 pm respectively. The N…H hydrogen bonding decreases the electron density in the binding region of the O1—H1 and O2—H2 bonds. Hence, the O1—H1 and O2—H2 bonds (100.2 pm), which are not engaged in the intramolecular H-bonds, are longer than the O3—H4 and O4—H9 bonds (96.6 pm).

As seen in Fig. 2, deprotonated L^{2-} acts as a dianionic tetradentate ligand that has an N, N, O^-, O^- binding mode via the deprotonated phenolic oxygens and the azomethine nitrogen atoms. In the structure of the Mn(II) complex, four coordinated atoms are roughly in the same plane together with the Mn^{2+} ion. The calculated O2—N2—N1—O1 and O1—O2—N2—Mn dihedral angles are –6.5° and 2.4° respectively.
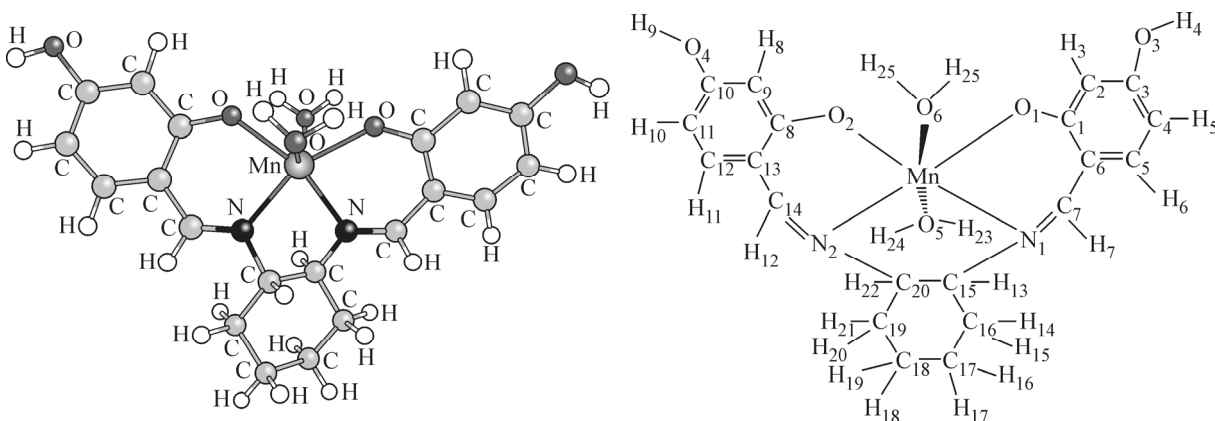

Fig. 2. Structure and B3LYP optimized geometry of the $[Mn(L)(H_2O)_2]$ complex together with its labeling

The benzene rings rotate around the C15—N1 and C20—N2 single bonds which put them in the same plane. This provides structural requirements for the complex formation. Therefore, the complexation results in a considerable decrease in the O1—O2 and N1—N2 distances, from 657.8 pm and 297.1 pm for H_2L to 359.0 pm and 273.8 pm for the Mn complex respectively.

The coordinated ligand is more planar than the free one. Going from the free ligand to the complex, the N1—C15—C20—N2, O1—N1—N2—O2 and C1—C7—C14—C8 dihedral angles vary from 70.9°, 107.2°, and 116.0° to 52.1°, 27.2°, and 25.3° respectively. In the complex structure, the C2—C6—C13—C9 and C3—C5—C12—C10 dihedral angles of the Mn complex are 24.9° and 25.2° respectively.

The deprotonation of phenolic O1 and O2 oxygen atoms results in a decrease of the C1—O1 and C8—O2 bond lengths in the complex by 4.1 pm, in comparison with the free H_2L ligand (134.0 pm). However, the C3—O3 and C10—O4 bond lengths are about 136 pm in both free and coordinated ligand.

Both of the C15—N1 and C20—N2 bond lengths (145.8 pm and 147.5 pm for the ligand and the complex respectively) are of appropriate size for the single C—N bond, while both azomethine C7—N1 and C14—N2 (128.8 pm to 129.1 pm for the ligand and the complex respectively) correspond to the double C=N bond. The C7=N1 and C14=N2 bonds are in the same plane with the corresponding benzene rings. For example, the C1—C6—C7—N1 and C7—C6—C5—C4 dihedral angle is –0.68° and 177.9° in the free ligand, and 2.5° and 180.0° in the coordinated ligand respectively. The coordination of nitrogen atoms to Mn^{2+} results in the elongation of the C—N bonds of the ligand.

In the octahedral structure of the Mn comlex, the O1, O2, N1, and N2 atoms of the L^{2-} ligand occupy the equatorial positions, while the two axial positions are occupied by two H_2O ligands. The Mn—O1 and Mn—O2 bond lengths are 210.5 pm and 210.4 pm respectively, which are shorter than the Mn—N1 (220.5 pm) and Mn—N2 (220.3 pm) bond lengths.

The axial Mn—O bonds (H_2O ligands) are longer than the equatorial ones (the Schiff-base ligand), where the calculated Mn—O5 and Mn—O6 bond lengths are about 238.5 pm. The calculated O5—Mn—O6, O5—Mn—N1, and O5—Mn—O1 angles are 134.7°, 98.8°, and 84.1° respectively, demonstrating that the axial H_2O ligands are not completely perpendicular to the equatorial plane of the distorted octahedral complex. The DFT calculated parameters for the investigated H_2L ligand and its Mn complex are consistent with the previously reported data for the similar salen ligands and complexes [25—35].

Chemistry. In the present work, the H_2L Schiff-base and the octahedral $[Mn^{II}(L)(H_2O)_2]$ complex were newly synthesized and characterized by the elemental analysis and IR and NMR spectroscopies.

Elemental analysis. The elemental analysis results for the H_2L ligand (Anal. Calcd. for $C_{20}H_{20}N_2O_4$: C, 67.87; H, 6.26; N, 7.90. Found: C, 67.69; H, 4.89; N, 8.29 %) and the $[Mn(H_2O)_2L]$ complex (Anal. Calcd. for $C_{20}H_{22}N_2O_6Mn$: C, 52.50; H, 4.82; N, 6.07 %. Found: C, 52.95; H, 5.96; N, 6.17 %.) confirm the proposed formulas.

NMR spectra of H_2L. In Table 1, the experimental and computational ^1H and ^{13}C NMR chemical shifts (δ) of the H_2L ligand are listed, where the atomic positions are numbered as in Fig. 1. The DFT chemical shifts are in good agreement with the experimental values, confirming the validity of the optimized geometry for H_2L. The only exceptions are the H4 and H9 hydrogen atoms, where the computed chemical shifts are significantly lower than the experimental ones. It is notable that the experimental data are from $(CD_3)_2CO$ solutions; while the calculated results correspond to the isolated molecule in the gas phase. Obviously, the solvent molecules interact with the —OH protons. In addition, the H4 and H9 atoms can be engaged in intermolecular hydrogen bonds.

The appearance of a signal at 13.13 ppm is attributed to the H1 and H2 phenolic protons (H1, H2) where their engagement in the intramolecular-hydrogen-bond interaction (O—H…N) shifts their signals upfield [12—15, 39].

Vibrational spectroscopy. Nowadays, a theoretical assignment of the spectra is used as an useful tool for the identification of chemical compounds [11—15, 21—24, 40]. Here, the vibrational modes were analyzed by comparing the DFT and experimental IR spectra. The assignment of the selected vibrational wavenumbers of the H_2L ligand and its complex are gathered in Table 2.

T a b l e   1

Experimental and DFT calculated ^{1}H- *and* ^{13}C-NMR *chemical shifts of* 3,3′-*dihydroxy*-4,4′-
[1,2-*cyclohexanediyl bis* (*nitrilomethylidyne*)]-*bis-phenol ligand in the* $(CD_3)_2CO$ *solution*, δ (ppm)

Atomic position	Exp.	Theor.	Atomic position	Exp.	Theor.	Atomic position	Exp.	Theo.	Atom position	Exp.	Theor.
				^{1}H NMR				^{13}C NMR			
H1	13.60	13.13	H10	6.12	5.82	C1	165.0	172.53	C4	107.2	106.56
H2	13.60	13.13	H22	3.30	3.97	C8	165.0	171.39	C11	107.2	106.46
H9	9.60	3.79	H13	3.30	3.48	C7	164.1	168.52	C2	102.7	106.36
H4	9.60	3.72	H14		2.22	C14	164.1	168.43	C9	102.7	106.36
H7	8.27	8.13	H18	1.76—1.88	1.99	C10	161.9	166.91	C15	70.8	75.23
H12	8.27	8.13	H19, H20		1.85	C3	161.9	166.51	C20	70.8	63.66
H6	7.12	6.89	H15		1.75	C5	133.5	137.96	C16	33.1	34.66
H11	7.12	6.89	H21	1.41—1.53	1.68	C12	133.5	137.35	C17	24.1	23.06
H3	6.23	6.45	H17		1.60	C6	111.5	117.93	C19	24.1	22.96
H8	6.23	6.57	H16		1.54	C13	111.5	117.93	C18	24.1	22.36
H5	6.12	5.82									

T a b l e   2

Selected experimental and calculated IR vibrational frequencies (cm^{-1}) *of the*
3,3′-*dihydroxy*-4,4′-[1,2-*cyclohexanediyl bis*(*nitrilomethylidyne*)]-*bis-phenol ligand and its* Mn(II) *complex*

Experimental frequencies		Calculated frequencies		Vibrational assignment
Ligand	Mn Complex	Ligand	Mn Complex	
—		—	616	δ_{wag}(O—H) H_2O
		869	—	δ_{op}(O1—H1,O2—H2)
850 (m)	850 (m)	957	960	Breathing of benzene rings
1180 (s)	1150 (m)	1029	977	υ(C15—N1, C20—N2)
		1111—1137	1108—1133	δ_{ip}(aromatic hydrogens)
		1194		δ_{op}(O3—H4,O4—H9)
1280 (s)	1280 (s)	1218	1198	υ(C3—O3, C10—O4, C6—C7, C13—C14)
1365 (s)	1375 (s)	1377	1382	δ_{ip}(C7—H7,C14—H12)
1400 (m)	1410 (m)	1437	1429	υ(C1—O1, C8—O2)
1473 (vs)	1475 (vs)	1507	1502	υ_{sym}(C=C) benzene rings
	1516 (m)	—	1555	δ_{sci}(OH) H_2O
1630 (vs)	1615 (vs)	1626	1590	υ_{asym}(C=C) benzene rings
		1630	1594	υ(C7=N1, C14=N2)
2930(s),	2930(s),	2879—2960	2870—2936	υ(CH) cyclohexane ring
3450(br)	3450(br)	2961	2951	υ(C7—H7,C14—H12)
		2964	—	υ(O1—H1, O2—H2)
		3065—3105	3027—3073	υ(C—H) aromatic
		3674	3685	υ(O3—H4, O4—H9)
		—	3528	υ_{sym}(O—H) H_2O
		—	3805	υ_{asym}(O—H) H_2O

Abbreviation: sci, scissoring; wag, wagging; op, out-of-plane; ip, in-plane; w, weak; m, medium; s, strong; vs, very strong; br, broad.

In the 3600—2000 cm^{-1} spectral region of the IR spectra, the overlapping of stretching vibrations of the O—H bonds with each other and with the C—H stretching modes leads to a band broading [12—15, 41, 42], the deconvolution of which is given in Table 2. In the ligand spectrum, the most intense band is attributed to the stretching vibrations of the O1—H1 and O2—H2 bonds. These vibrations appear at much lower energies than the corresponding vibrations for the O3—H4 and O4—H9 bonds, which can be attributed to the engagement of H1 and H2 in the intramolecular hydrogen bond interaction. For the spectrum of the complex, the most intense band appears at 3527 cm^{-1}, which can be attributed to the symmetric O—H stretching vibration of the H_2O species.

An important diagnostic for the coordination mode of Schiff-bases is the energy value of the very intense band in the 1660—1500 cm^{-1} region of the IR spectra [12—15, 41—43], which is related to the azomethine C=N bonds. By complexation, the symmetrical stretching modes of C7=N1 and C14=N2 bonds shift to lower energy by 15 cm^{-1} in comparison with the free H_2L ligand (1630 cm^{-1}), confirming the coordination of H_2L through the azomethine nitrogen atoms (N1 and N2) [12—15, 41, 42]. In the complex spectrum, the scissoring vibrational mode of the H_2O molecule is overlapped by this intense band.

By complexation, the stretching vibrations of the C1—O1 and C8—O2 bonds (at 1400 cm^{-1}) shift to higher frequencies by 10 cm^{-1}, demonstrating that the electron density in the bonding region of C1—O1 and C8—O2 is increased by the deprotonation and coordination of O1 and O2 phenolic oxygen atoms.

The obtained computational data could be useful for the identification of similar compounds, which involves the structural parameters of the investigated species and the assignment of their vibrational frequencies and NMR chemical shifts.

CONCLUSIONS

Here, the H_2L Schiff-base ligand and its $[Mn(L)(H_2O)_2]$ complex have been newly synthesized and characterized by the elemental analysis, NMR and IR spectroscopies. The proposed formulas for both ligand and complex are in agreement with the experimental results.

The newly synthesized species were investigated computationally using the DFT methods. The optimized geometry of the H_2L ligand is not planar. In the Mn complex, L^{2-} acts as a dianionic ligand coordinated to the Mn^{2+} ion with N, N, O$^-$, O$^-$ donor sites of resorcinol OH and azomethine N. The four coordinating atoms of L^{2-} occupy the equatorial positions of the octahedral complex, while the axial positions are occupied by two H_2O ligands. The optimized geometry of the complex is significantly more planar than that of the free ligand.

In the free ligand, the H1 and H2 phenolic protons are engaged in the intramolecular hydrogen bond (—O—H…N), which affects considerably their NMR chemical shifts and energy of their O—H stretching vibration in the IR spectra, too.

The computed parameters are in good agreement with the values reported for the similar compounds. On the other hand, the DFT calculated IR frequencies and NMR chemical shifts also confirm the experimental data, showing the validity of the optimized geometries for the investigated species.

REFERENCES

1. *Sevvel R., Rajagopal S., Srinivasan C., Ismail Alhaji N., Chellamani A.* // J. Org. Chem. – 2000. – **65**. – P. 3334 – 3340.
2. *Meunier B.* // Chem. Rev. – 1992. – **92**. – P. 1411 – 1456.
3. *Ostovic D., Bruice T.C.* // Acc. Chem. Res. – 1992. – **25**. – P. 314 – 320.
4. *Canali L., Sherrington D.C.* // Chem. Soc. Rev. – 1999. – **28**. – P. 85 – 93.
5. *Bahramian B., Mirkhani V., Moghadam M., Amin A.H.* // Appl. Catal. A: General. – 2006. – **315**. – P. 52 – 57.
6. *Palucki M., McCormick G.J., Jacobsen E.N.* // Tetrahedron Lett. – 1995. – **36**. – P. 5457 – 5460.
7. *Irie R., Hosoya N., Katsuki T.* // Synlett. – 1994. – P. 255 – 256.
8. *Linker T.* // Angew. Chem., Int. Ed. Engl. – 1997. – **36**. – P. 2060 – 2062.

9. *Hamada T., Fukuda H., Katsuki T.* // Tetrahedron. – 1996. – **52**. – P. 515 – 530.

10. *Gravert D.J., Griffin J.H.* // Inorg. Chem. – 1996. – **35**. – P. 4837 – 4847.

11. *Routier S.E., Bernier J.L., Warninig M.J., Colson P., Bailly C.* // J. Org. Chem. – 1996. – **61**. – P. 2326 – 2331.

12. *Eshtiagh-Hosseini H., Housaindokht M.R., Beyramabadi S.A., Beheshti S., Esmaeili A.A., Javan Khoshkholgh M., Morsali A.* // Spectrochim. Acta Part A: Molecular and Biomolecular Spectroscopy. – 2008. – **71**. – P. 1341 – 1347.

13. *Eshtiagh-Hosseini H., Housaindokht M.R., Beyramabadi S.A., Mir Tabatabaei S.H., Esmaeili A.A., Javan Khoshkholgh M.* // Spectrochim. Acta Part A: Molecular and Biomolecular Spectroscopy. – 2011. – **78**. – P. 1046 – 1050.

14. *Beyramabadi S.A., Morsali A., Javan Khoshkholgh M., Esmaeili A.A.* // Spectrochim. Acta Part A: Molecular and Biomolecular Spectroscopy. – 2011. – **83**. – P. 467 – 471.

15. *Beyramabadi S.A., Morsali A., Javan Khoshkholgh M., Esmaeili A.A., Vahidi S.H.* // J. Struct. Chem. – 2012. – In press.

16. *Lee C., Yang W., Parr R.G.* // Phys. Rev. B. – 1988. – **37**. – P. 785 – 789.

17. *Frisch M.J. et al.* Gaussian 98, Revision A.7; Gaussian, Inc.: Pittsburgh PA, 1998.

18. *Hay P.J., Wadt W.R.* // J. Chem. Phys. – 1985. – **82**. – P. 299 – 310.

19. *Ditchfield R.* // Mol. Phys. – 1974. – **27**. – P. 789 – 807.

20. *Young D.C.* Computational Chemistry: A Practical Guide for Applying Techniques to Real – World Problems, John Wiley & Sons, Inc., 2001.

21. *Beyramabadi S.A., Morsali A., Vahidi S.H.* // J. Struct. Chem. – 2012. – In press.

22. *Takjoo R., Centore R., Hakimi M., Beyramabadi S.A., Morsali A.* // Inorg. Chim. Acta. – 2011. – **371**. – P. 36 – 41.

23. *Özdemir N., Dayan O., Dinçer M., Çetinkaya B.* // J. Struct. Chem. – 2012. – **53**. – P. 251 – 259.

24. *Proft F.D., Geerlings P.* // Chem. Rev. – 2001. – **101**. – P. 1451 – 1464.

25. *Karabiyik H., Güzel B., Aygün M., Boga G., Büyükgüngör O.* // Acta Crystallogr. – 2007. – **C63**. – P. o215 – o218.

26. *Abu-Surrah A.S., Laine T.V., Repo T., Fawzi R., Steimann M., Rieger B.* // Acta Crystallogr. – 1997. – **C53**. – P. 1458 – 1459.

27. *Li X.-Z., Qu Z.-R.* // Acta Crystallogr. – 2008. – **E64**. – P. o848.

28. *Li X.-Z., Qu Z.-R.* // Acta Crystallogr. – 2008. – **E64**. – P. o1121.

29. *Srinivasan K., Michaud P., Kochi J.K.* // J. Amer. Chem. Soc. – 1986. – **108**. – P. 2309 – 2320.

30. *Ma C.-B., Chen F., Chen C.-N., Liu Q.-T.* // Acta Crystallogr. – 2003. – **C59**. – P. m516 – m518.

31. *Huang D.-G., Zhang X.-F., Zhu H.-P., Chen C.-N., Liu Q.-T.* // Acta Crystallogr. – 2001. – **E57**. – P. m441 – m443.

32. *Butcher R.J., Towns W.* // Acta Crystallogr. – 2005. – **E61**. – P. m2618 – m2620.

33. *Martínez D., Motevalli M., Watkinson M.* // Acta Crystallogr. – 2002. – **C58**. – P. m258 – m260.

34. *Ni Z.-H., Kou H.-Z., Zhang L.-F., Jiang Y.-B., Cui A.-L.* // Acta Crystallogr. – 2005. – **E61**. – P. m796 – m798.

35. *Suleiman Gwaram N., Khaledi H., Mohd Ali H.* // Acta Crystallogr. – 2010. – **E66**. – P. m813.

36. www.cambridgesoft.com/Ensemble_for_Chemistry/ChemDraw, Version ultra 8.0, 2003.

37. *Zhurko G.A., Zhurko D.A.* CHEMCRAFT, Version 1.6, 2010.

38. *Dal H., Süzen Y., Şahin E.* // Spectrochim. Acta Part A. – 2007. – **67**. – P. 808 – 814.

39. *Pui A., Policar C., Mahy J.-P.* // Inorg. Chim. Acta. – 2007. – **360**. – P. 2139 – 2144.

40. *Eshtiagh-Hosseini H., Aghabozorgb H., Mirzaei M., Beyramabadi S.A., Eshghi H., Morsali A., Shokrollahi A., Aghaei R.* // Spectrochim. Acta Part A. – 2011. – **78**. – P. 1392 – 1396.

41. *Sanmartín J., García-Deibe A.M., Fondo M., Navarro D., Bermejo M.R.* // Polyhedron. – 2004. – **23**. – P. 963 – 967.

42. *Ware D.C., Mackie D.S., Brothers P.J., Denny W.A.* // Polyhedron. – 1995. – **14**. – P. 1641 – 1646.

43. *Khandar A.A., Shaabani B., Belaj F., Bakhtiari A.* // Polyhedron. – 2006. – **25**. – P. 1893 – 1900.